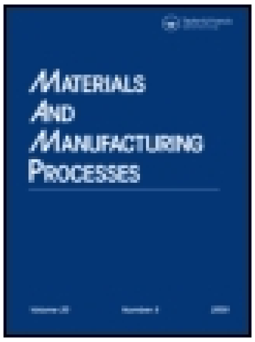

Taylor & Francis
Taylor & Francis Group

Materials and Manufacturing Processes

ISSN: 1042-6914 (Print) 1532-2475 (Online) Journal homepage: http://www.tandfonline.com/loi/lmmp20

Reactive Synthesis of Aluminide Intermetallics

David C. Dunand

To cite this article: David C. Dunand (1995) Reactive Synthesis of Aluminide Intermetallics, Materials and Manufacturing Processes, 10:3, 373-403, DOI: 10.1080/10426919508935033

To link to this article: http://dx.doi.org/10.1080/10426919508935033

Materials and Manufacturing Processes Vol. 10, No. 3, 373-403, 1995

Reactive Synthesis of Aluminide Intermetallics

David C. Dunand
Department of Materials Science and Engineering
Massachusetts Institute of Technology
Cambridge, MA 02139, USA.

Abstract

Reactive synthesis of bulk and reinforced aluminides are reviewed. When processed under optimal conditions, reactively-synthesized aluminides display room-temperature mechanical properties as good as, or better than, cast aluminides. Frequently encountered defects resulting from reactive synthesis are: (i) porosity, (ii) incomplete synthesis and (iii) loss of shape due to liquid formation. Using a simple mass balance, the amount of liquid aluminide is calculated as a function of the initial temperature of the reactants. Process maps are discussed for some of the aluminides of nickel and titanium.

1.0 Introduction

Recently, considerable interest has been directed to the reactive synthesis of intermetallic compounds. While the technique has been used since the beginning of the century for oxide-metal mixtures (thermite reaction), it was pioneered for intermetallics in the Soviet Union in the 1970's (1-3). In reactive processing of intermetallics, two intimately-mixed metallic reactants A and B exothermically react in a self-sustaining manner to form an intermetallic product A_xB_y, as a result of the large difference in free energy and enthalpy between the product and reactants:

$$x\,A + y\,B \rightarrow A_xB_y \qquad (1)$$

The number of reactants and/or products can be larger than shown in Eq. (1), and non-elemental reactants, e.g. in displacement reactions, can be used:

$$AC_y + x\,B \rightarrow AB_x + y\,C \qquad (2)$$

Compared to other processes such as casting and powder metallurgy of prealloyed powders, reactive synthesis has the following advantages:

- reduction in externally-supplied energy, since the enthalpy released by the reaction internally heats the product. This in turn reduces or eliminates the need for processing equipment such as furnaces.

- rapid heating and cooling rates, resulting in short production cycles, fine-grained microstructures, and reduced contamination from reaction with the surroundings (atmosphere, reinforcement or crucible materials). The rapid heating is a result of (i) the heat being released within the volume of the reactant preform, rather than conducted from its surface, as in most external heating methods, and (ii) high density of stored chemical energy being liberated in a self-sustaining manner. Rapid cooling may be induced by initiating the reaction at low temperature and keeping the product in contact with cold surroundings.
- high purity of the product, due to evaporation of volatile impurities at the high temperatures reached during synthesis.
- possibility to produce composites, either by *in situ* formation of a second phase or by addition of an inert second phase to the reactants.
- possibility of near-net-shape processing, particularly useful for intermetallics and their composites, which are difficult to shape due to their limited low-temperature ductility, and difficult to cast due to their high melting point and reactivity.

Some of the disadvantages of reactive synthesis processing include:

- difficulty of controlling the reaction kinetics once synthesis has been initiated,
- the use of powders, which may increase contamination as a result of their large specific area, and are inherently more expensive than melts,
- final porosity in the product, which can however be minimized or eliminated by application of pressure during or after reaction,
- loss of shape for self-standing preforms as a result of slumping upon melting, swelling upon gas evolution, or shrinking upon densification, and
- loss of volatile reactants or products.

The large body of work existing on the reactive synthesis processing of ceramics and intermetallics has been summarized in numerous review articles, e.g. refs. (1-14). In what follows, a review of the literature relative to reactive synthesis of aluminide intermetallics and their composites is presented.

2.0 Reactive Synthesis Processes

In many cases of reactive synthesis, partial or complete melting of some of the species involved in the reaction (reactants, intermediate or final products) takes place. Formation of a liquid phase is advantageous, since densification is accelerated due to capillary forces, and mass transport is much faster than in the solid state. Liquid formation may also be disadvantageous, since it may induce a loss of shape of the sample and segregation. Furthermore, since the enthalpy of fusion of the melted species is absorbed without increase in overall temperature, the maximum temperature of the product is reduced, thus increasing the possibility of incomplete reaction.

The maximum temperature reached during adiabatic reactive synthesis is mostly controlled by the amount of liquid reactants at the beginning of the reaction, since the enthalpy of fusion of the reactants is usually high compared to the total enthalpy needed to bring the reactants from their initial temperature to the final temperature of the reaction. Thus, current reactive synthesis processes can be separated in three classes, according to the physical state of the reactants at the onset of the reaction (Figure 1).

2.1 Class (i): All Reactants Are Solid

- *Self-propagating High-temperature Synthesis (SHS)*: a mixture of reactant materials is compacted into a porous, self-supporting preform. The preform is subjected to a localized temperature increase (e.g., torch, electric arc), initiating locally the reaction which propagates in a front through the preform.
- *Reactive Sintering (RS)*: a porous preform of reactant materials is heated uniformly until a self-sustaining reaction takes place simultaneously within its volume.
- *Reactive Annealing (RA)*: similar to reactive sintering, except that the mixture of reactants is a pore-free body (produced by lamination of foils, extrusion of powders or infiltration of preforms).
- *Reactive Hot Isostatic Pressing (RHIP):* similar to reactive sintering, except that hydrostatic pressure is imposed onto the reacting preform, thus compacting the product.
- *Reactive Hot Pressing (RHP)*: similar to reactive HIPing, except that a uniaxial compressive stress is applied mechanically by a piston onto the preform which is usually contained within a die.
- *Reactive Shock Synthesis (RSS)*: a porous preform of reactant powder is subjected to a very rapid increase of pressure and temperature as a result of a shock wave, thus initiating a self-sustaining reaction leading to the products.

2.2 Class (ii): Some Reactants Are Liquid

- *Reactive Infiltration (RI)*: a preform of solid reactant materials is infiltrated with a fully liquid reactant, and the two react to form the product.

2.3 Class (iii): All Reactants Are Liquid

- *Reactive Spray Deposition (RSD)*: reactant powders are injected into, and melted within, a stream of inert hot gases or plasma, and deposited upon a substrate where they react to form the product.
- *Reactive Casting (RC)*: two streams of reactant liquid are mixed, and reacted in the liquid state to form the product.

Two other processes, where the product is also formed as a result of a reaction between reactants, are not considered in what follows, since the synthesis reaction is typically not self-sustaining:

- *Reactive Mechanical Alloying*: reactant powders are intimately mixed by repeated cold welding and fracture, resulting in diffusion of the reactants to form the product.
- *Reactive Deposition*: gaseous reactants are deposited onto a substrate where the product is synthesized.

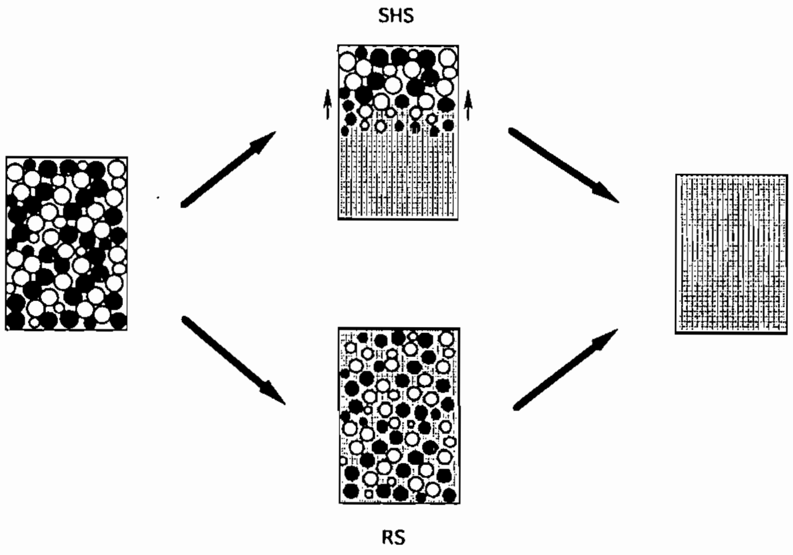

Reactive Powder Metallurgy
Class (i)

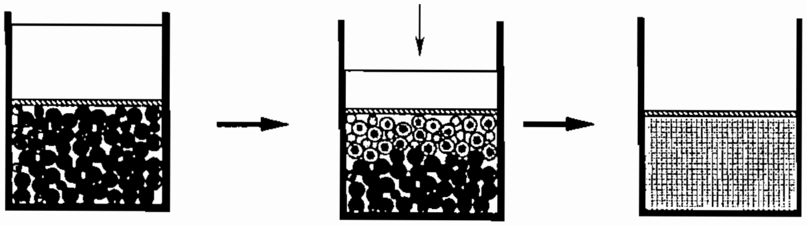

Reactive Infiltration
Class (ii)

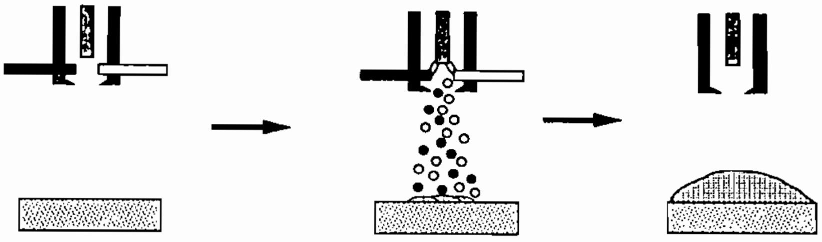

Reactive Spray Deposition
Class (iii)

Figure 1: Schematics of reactive synthesis processes.

3.0 Reactive Synthesis of Aluminides

The bulk of published research on reactive synthesis of intermetallics concerns aluminides and, to a lesser extent, silicides, which exhibit high strength, low density and good oxidation resistance. The two main problems for the use of these intermetallics for structural applications, i.e., their low ductility and toughness at room temperature and their low strength at elevated temperatures (15), have led to the development of composite systems, where the reinforcement can increase both toughness (by crack deflection, bridging or absorption) and strength (by load transfer) (16-19).

As compared to reactive synthesis of covalent or ionic ceramics (e.g., borides, carbides, nitrides and oxides), reactive synthesis of aluminides exhibits the following differences:

(a) Aluminum has low melting point and enthalpy of fusion, and forms eutectics with all aluminide-forming metals (20).
(b) Aluminides exhibit lower melting points than ceramics.
(c) The heat of formation of aluminides tends to be lower than for ceramics.
(d) The phase diagrams of all binary aluminum-transition metals systems exhibit multiple intermetallic phases (20), which often possess similar enthalpy and free energy of formation.
(e) Most aluminides tend to react with oxygen, and, to a lesser extent, nitrogen or carbon at high temperatures when in the solid or liquid state.

Journal articles up to 1993 are listed in Appendices 1-4 for bulk and reinforced aluminides fabricated by reactive synthesis. Also given in Appendices 1-4 is a summary of the process conditions, the microstructure of the products (phases and porosity), and, when available, their mechanical properties at room temperature.

It is apparent from Appendices 1-4 that dense, fully-reacted aluminides exhibit room-temperature mechanical properties which are as good as, and often better than, cast aluminides. This is probably due to the higher purity of the product, and the fine-grain structure resulting from rapid cooling. As for conventionally-produced aluminides, the properties of reaction-synthesized aluminides can further be modified by heat-treatment and thermo-mechanical treatments. Appendices 1-4 also indicate that the three main processing problems encountered during reaction synthesis of aluminides are porosity, incomplete reaction and loss of shape, as described in more detail below.

3.1 Porosity

Porosity, which can be minimized or eliminated by application of pressure during or after reaction, is induced by the following factors (21):

- Initial porosity of the reactant body: powder preforms exhibit 20-50 vol% porosity. Full green density is only reached upon reactive annealing of pore-free laminated, extruded or infiltrated preforms, or upon reactive infiltration.
- Decrease in molar volume upon formation of the product: for aluminides, the increase in density is typically less than 12% (Table 1), i.e.,

less than for most ceramics (10-30%).

- Thermal migration in temperature gradients (Soret effect): this is only of concern for SHS reactions where large gradients exist.
- Liberation of gases: powders of reactive metal (e.g., titanium, zirconium and niobium) dissolve large quantities of hydrogen, oxygen and nitrogen at low temperatures. These gases can be released during high-temperature synthesis and trapped within the product. Furthermore, chemically-bonded water on the surface of alumina used for composite has been found to desorb and react during synthesis of titanium aluminides (22).
- Solidification shrinkage: when liquid aluminide is formed, pores may result from lack of feeding of the solidification shrinkage.

3.2 Incomplete Reaction

Factors (c) and (d) above indicate that metastable intermetallic phases may form upon reactive synthesis of aluminides due to an insufficient maximum temperature. Low reactant initial temperature, non-stoichiometric composition and addition of non-reactive species (e.g., reinforcement) reduce the maximum attainable temperature. Also, if the reaction is non-adiabatic, low preform green density and large reactant particle size reduce the rate of reaction, thus increasing the heat losses to the surroundings, and reducing the final temperature. Furthermore, high surface-to-volume ratio of the reacting body also increase heat losses with the same results.

3.3 Loss of Shape

From factors (a) and (b) above, it follows that liquid formation is often encountered during reactive synthesis of aluminides, either because of formation of a transient liquid (aluminum or aluminum-eutectic) or because of melting of the aluminide at the maximum reaction temperature.

The final temperature of the product is of practical importance, since it helps in predicting the extent of reaction with the surroundings (atmosphere, crucible or inert reinforcement within the reactants), as well as the presence of liquid aluminide product. If partial or complete melting of the intermetallic product occurs, it is furthermore important to determine the volume fraction of liquid: this parameter determines the extent of shape deformation if no crucible is used, the extent of particle segregation due to density mismatch if a composite preform is used, as well as the extent of shrinkage porosity that must be fed during solidification. The conditions leading to melting of the product are further examined below: a simple thermodynamic analysis to determine the volume fraction of liquid product formed under adiabatic conditions is presented as a function of the initial reactant temperatures.

4.0 Global Adiabatic Thermodynamical Analysis

Calculations of the maximum temperature (also called adiabatic temperature) and volume fraction of liquid product have been presented for some ceramic systems (25-27) assuming adiabatic conditions, which have been found to be met in many SHS cases, since the synthesis reaction is typically fast (2).

While in class (i) of reactive synthesis processes, the initial temperature of the reactants is uniform, in reactive infiltration (class (ii)) and reactive casting (class (iii)), the temperature of the reactants can be controlled independently. This introduces additional flexibility in the process, since the initial temperature of the reactants is one of the main parameters that determines the final temperature of the reacted compounds, and therefore the amount of liquid product.

The volume fraction V_l of liquid product formed from the reactants A and B, initially at temperature T_A and T_B respectively, can be determined from a simple thermal balance consideration, if it is assumed that the process is adiabatic and that the product forms homogeneously throughout the sample according to Eq. (1):

$$x\left(\int_{T_A}^{T_m} c_{p,A}dT + \sum \delta_A \cdot \Delta H_{t,A}\right)$$
$$+y\left(\int_{T_B}^{T_m} c_{p,B}dT + \sum \delta_B \cdot \Delta H_{t,B}\right)$$
$$+ v_l \Delta H_{m,A_xB_y} + \Delta H_{f,A_xB_y} = 0 \tag{3}$$

where $c_{p,i}$ is the heat capacity of reactant i, $\Delta H_{t,i}$ is the enthalpy of transformation of reactant i (solid-solid and solid-liquid phase transformations), $\Delta H_{m,AxBy}$ and $\Delta H_{f,AxBy}$ are respectively the enthalpy of fusion and the enthalpy of formation of the solid product at its melting point T_m. Depending on the value of the phase transformation temperature $T_{t,i}$ of reactant i, the parameters δ_i takes the following values:

$\delta_i = 1$ if $T_i < T_{t,i} < T_m$, or

$\delta_i = 0$ if $T_i > T_{t,i}$ or $T_{t,i} > T_m$, or

$0 < \delta_i < 1$, if $T_i = T_{t,i}$ or $T_{t,i} = T_m$. (4)

Equation (3) can be adapted to more complex cases, e.g. when a larger number of reactants and products are involved in the reaction, when the reactants are compounds rather than metals (Eq. (2)), when the reaction is incomplete or yields non-equilibrium intermediate products, when a non-reactive species is added to the system or when the intermetallic product is non-stoichiometric (28, 29).

As shown schematically in Figure 2, Eq. (3) can be represented in a process map as a family of curves for which the volume fraction of liquid product V_l is constant (isofractional curves), as a function of the initial temperatures of the reactants T_A and T_B. The curves $V_l = 0$ and $V_l = 1$ bound a region (B) where the product is partially liquid at its melting temperature T_m. Adjacent to this region are two regions: a solid region (A), where the adiabatic temperature is below T_m, and a liquid region (C) where it is above T_m. The transformation temperatures of the reactants correspond to discontinuities on the isofractional curves, due to the enthalpies of transformation in Eq. (3).

The process region for class (i) of reactive synthesis, whereby all reactants are initially solid, is the line defined by:

$$T_A = T_B < T_{m,A} \text{ or } T_{m,b} \tag{5}$$

Class (ii) of reactive synthesis (reactive infiltration) is represented by the two areas defined by:

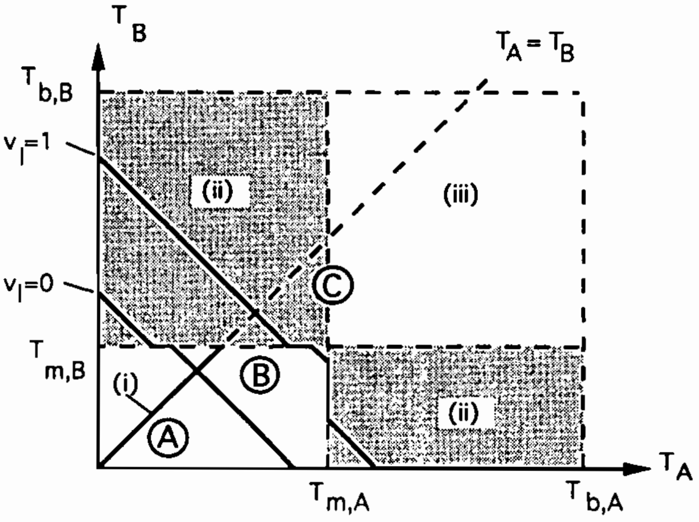

Figure 2: Schematic process map with process regions as a function of the initial temperature of the reactants.

$$0 < T_A < T_{m,A} \text{ and } T_{m,B} < T_B < T_{b,B}, \text{ or}$$
$$0 < T_B < T_{m,B} \text{ and } T_{m,A} < T_A < T_{b,A}, \quad (6)$$

where $T_{m,i}$ and $T_{b,i}$ are respectively the melting and boiling temperature of reactant i. The special case of isothermal reactive infiltration, where the liquid B and the solid A have the same temperature, corresponds to the line $T_A = T_B$ above the melting temperature of the lowest melting reactant. Finally, the area

$$T_{m,A} < T_A < T_{b,A} \text{ and } T_{m,B} < T_B < T_{b,B} \quad (7)$$

corresponds to class (iii) of reactive synthesis processes, where both reactants are initially liquid.

5.0 Examples of Process Maps for Titanium and Nickel Aluminides

In Figures 3-6, Eq. (3) is plotted in process maps for the products TiAl, $TiAl_3$, NiAl and Ni_3Al, using thermodynamic data given in Table 1 and ref. (23). Figure 3 for TiAl displays isofractional curves which are almost straight and regularly spaced, as a result of the weak temperature dependence of the heat capacity of the two parent metals. When the phase transformation temperature of one of the reactants is reached (melting or endothermic allotropic transformation), the temperature of the other reactant is shifted to lower values for a constant fraction of liquid product V_l.

The following differences between the two titanium aluminides TiAl and $TiAl_3$ are visible in Figures 3 and 4: the shift in isofractional curves due to the melting of aluminum is larger in the case of $TiAl_3$ than for TiAl, while the shift due to the phase transformations of titanium (α-β and β-liquid) as well as the slope of the isofractional curves are smaller for $TiAl_3$

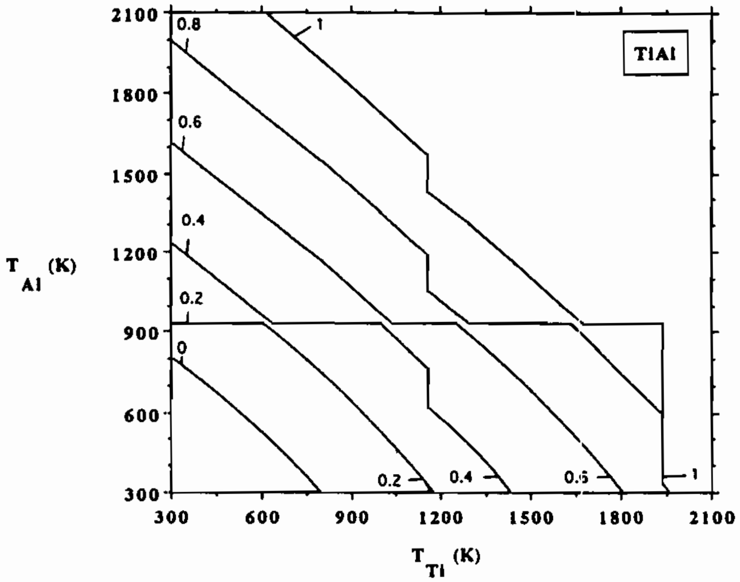

Figure 3: Plot of the volume fraction of liquid TiAl as a function of the reactant initial temperatures (Eq. 3).

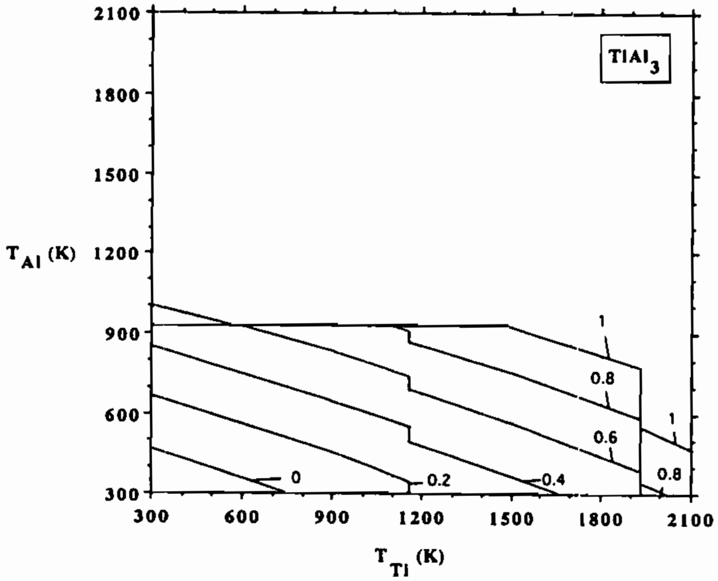

Figure 4: Plot of the volume fraction of liquid $TiAl_3$ as a function of the reactant initial temperatures (Eq. 3).

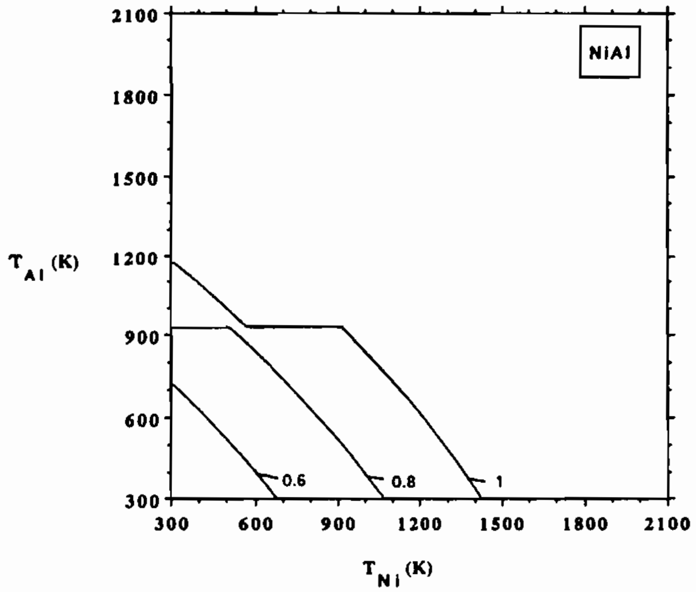

Figure 5: Plot of the volume fraction of liquid NiAl as a function of the reactant initial temperatures (Eq. 3).

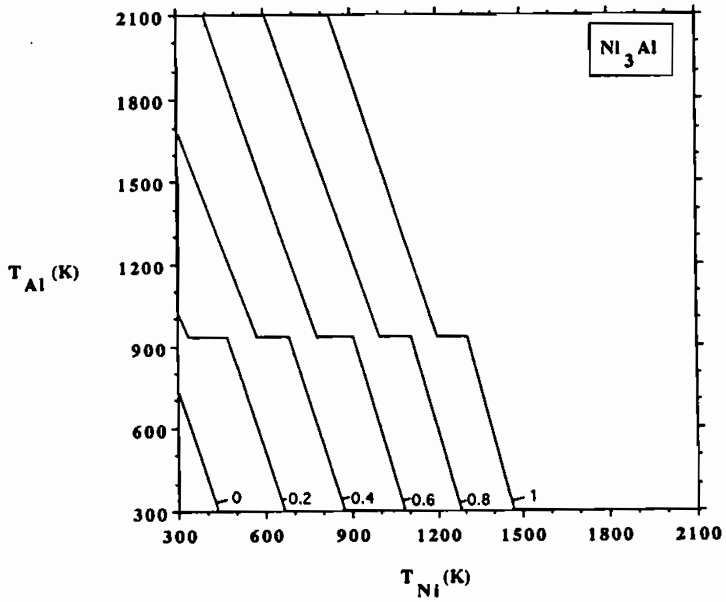

Figure 6: Plot of the volume fraction of liquid Ni_3Al as a function of the reactant initial temperatures (Eq. 3).

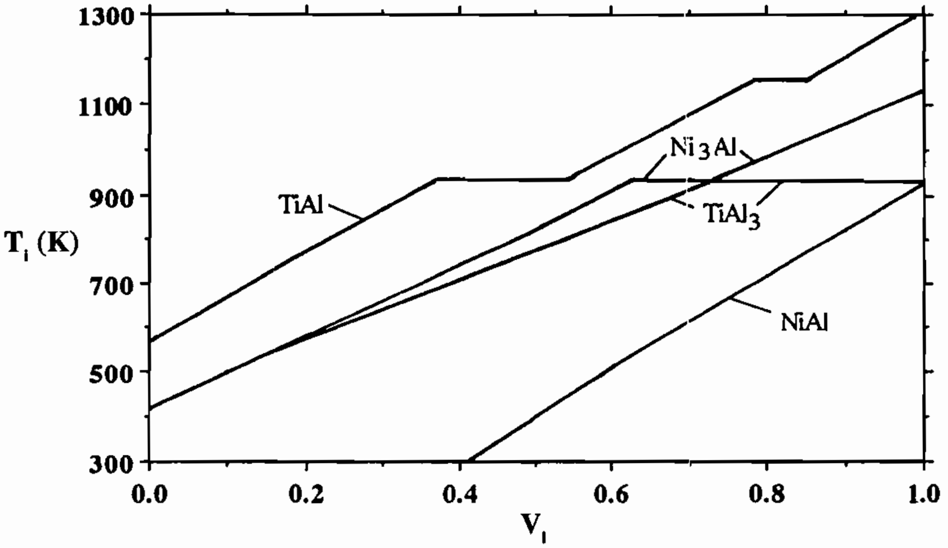

Figure 7: Plot of final volume fraction liquid product V_l as a function of the reactant temperature T_i for the case where both reactants are initially at the same temperature T_i (Eq. 3).

than for TiAl. These differences are the result of the different stoichiometry of the two compounds: a larger relative amount of aluminum is involved in the reaction to form $TiAl_3$ than for TiAl. Finally, compared to TiAl, the isofractional curves for $TiAl_3$ are shifted towards lower reactant temperatures. This can be explained by the ratio $-\Delta H_f/\Delta H_m$ which is higher for $TiAl_3$ than for TiAl (Table 1) and which represents the ratio of heat released by the reaction and heat absorbed upon melting of the intermetallic. It is a rough measure of the relative enthalpy source and sink of the system, since most of the enthalpy is used for melting the intermetallic rather than for heating the reactants.

Figure 5 shows isofractional curves for NiAl with about the same slopes as for TiAl (Figure 3), as a result of the similar stoichiometry, but shifted to lower reactant temperatures, as expected from the higher $-\Delta H_f/\Delta H_m$ ratio for NiAl. For Ni_3Al (Figure 6), the isofractional curves exhibit higher slopes with smaller aluminum melting plateaus than for NiAl (Figure 5). The reason for these differences is, as for the titanium aluminides, the different stoichiometric ratios of aluminum and nickel (respectively titanium).

The intersection of the isothermal line $T_A = T_B$ with the isofractional curves is plotted in Figure 7 for the intermetallics listed in Table 1. For all the aluminides considered, the melting point of the intermetallic is reached when both reactants are initially at the melting temperature of aluminum. The volume fraction of liquid intermetallic product depends on the volume fraction of liquid

Table 1. Thermodynamic Values (23, 24) Used in Calculation and Density Change $\Delta\rho$ upon Formation of the Intermetallic from the Metal Reactants

Compound	T_m (K)	ΔH_f at T_m (kJ/mol)	ΔH_m (kJ/mol)	$-\Delta H_f/\Delta H_m$ (-)	$\Delta\rho$ (kg/m^3)
TiAl	1733	-88	60	1.5	270
$TiAl_3$	1613	-182	80	2.3	230
NiAl	1912	-159	63	2.5	740
Ni_3Al	1668	-190	103	1.8	630

aluminum at the onset of the reaction: if the aluminum is fully solid at the start of the reaction (as for SHS of mixed powder preforms), then the volume fraction of liquid intermetallic is between 0.37 for TiAl and 1 for NiAl. If the aluminum is fully liquid before the initiation of the reaction (as in reactive infiltration of metallic powders), the liquid fraction of intermetallic takes values between 0.55 for TiAl and 1 for NiAl and $TiAl_3$. Due to the rapid and exothermic nature of reactive synthesis of direct measurement of the amount liquid formed at the maximum synthesis temperature is difficult. Indirect evidence of melting has been reported in three studies: Dunand and Mortensen (28) observed dendritic NiAl after reactive infiltration, indicating that a volume fraction of liquid NiAl close to unity was reached upon synthesis, Alman and Stoloff (30) reported slumping of reaction-sintered Ni-Al preforms as a result of NiAl melting, and Rawers and Maupin (31) observed shrinkage porosity in reactively-annealed nickel aluminides.

6.0 Summary

Reactive synthesis processes, whereby a product is formed by exothermic, self-sustaining reaction of reactants, are reviewed for aluminides and their composites. This class of processes allows rapid heating and cooling with little externally supplied heat, purification of the product as a result of the high temperature reached, and near-net-shape processing of bulk or reinforced products, whereby the reinforcement can be formed in situ or added to the reactants.

The main process defects encountered during reactive synthesis of aluminides are porosity, incomplete reaction and loss of shape. Porosity is common to most materials produced by reactive synthesis, and can be eliminated in aluminides by application of pressure during or after synthesis, since the intermetallics can usually be plastically deformed at high temperature. Incomplete reaction is more prevalent in aluminides than in ceramics, due to the comparatively low temperatures reached during synthesis. This in turn is due to the lower enthalpy of formation of aluminides, reducing the heat source, and the lower melting temperature of aluminum and aluminides, increasing the heat sink, since melting is endothermic. Loss of shape is mostly controlled by the amount of liquid aluminide product.

Using a simple mass balance equation, the volume fraction of liquid formed under equilibrium, adiabatic conditions is determined as a function of the initial temperature of the reactant metals. The results are displayed graphically in process maps and discussed for some of the aluminides of nickel and titanium, for which a large amount of liquid product can be formed upon reactive synthesis. While the adiabatic, equilibrium calculations yield an upper bound for the amount of liquid formed, they are relevant to practical cases, since full reaction has been usually found to take place when heat losses are small.

7.0 Acknowledgements

This work was sponsored by the National Science Foundation, through grant No. MSS-9201843 and by AMAX, through an endowed chair at MIT. The author wishes to thank Prof. A. Mortensen at MIT for helpful discussions.

8.0 References

1. Frankhouser, W. L., K. W. Brendley, M. C. Kieszek, and S. T. Sullivan, Gasless Combustion Synthesis of Refractory Compounds, Noyes Publishing, Park Ridge, NJ, (1985).
2. Merzhanov, A. G., Combustion and Plasma Synthesis of High-Temperature Materials, VCH, New York, p.1, (1990).
3. Merzhanov, A. G., Powder Metallurgy World Congress, Vol.9, Metal Powder Industries Federation, Princeton, NJ, p.341, (1992).
4. Munir, Z. A., Ceramic Bulletin, Vol.67, p.342, (1988).
5. Yi, H. C., and J. J. Moore, Journal of Materials Science, Vol.25, p.1159, (1990).
6. Stoloff, N. S., and D. E. Alman, MRS Bulletin, Vol.15, p.47, (1990).
7. Stoloff, N. S. and D. E. Alman, Materials Science and Engineering, Vol. A144, p. 51, (1991).
8. Rice, R. W., Journal of Materials Science, Vol.26, p.6533, (1991).
9. Subrahmanyam, J. and M. Vijayakumar, Journal of Materials Science, Vol.27, p.6249, (1992).
10. German, R. M., and R. G. Iacocca, Processing and Fabrication of Advanced Materials for High Temperature Applications - II, TMS, Warrendale, PA, p.93, (1992).
11. Munir, Z. A., Metallurgical Transactions, Vol.23A, p.7, (1992).
12. Wang, G. X., and M. Dahms, Powder Metallurgy International, Vol.24, p.219, (1992).

13. Munir, Z. A., Reviews in Particulate Materials, Vol.1, p.41, (1993).

14. Koczak, M. J., and M. K. Premkumar, Journal of Metals, Vol.45, p.44, (1993).

15. Stoloff, N. S., and C. T. Sims, Superalloys II, C.T. Sims, N.S. Stoloff, and W.T. Hagel, eds., John Wiley, New York, p.519, (1987).

16. LePetitcorps, Y., F. D. Martina, and J. M. Quenisset, Metal Matrix Composites-Processing, Microstructure and Properties, 12th Risø International Symposium on Materials Science, N. Hansen et al., eds., Risø National Laboratory, Roskilde, Denmark, p.461, (1991).

17. Anton, D. L., High Temperature/High Performance Composites, Vol.120, Materials Research Society, Pittsburgh, PA, p.57, (1988).

18. Amateau, M. F., and R. B. Bhagat, Advances in Powder Metallurgy & Particulate Materials - 1992, Vol.9, Metal Powder Industries Federation, Princeton, NJ, p.223, (1992).

19. Warren, R., ed., Ceramic-Matrix Composites, Blackie, Glasgow, (1992).

20. ASM Handbook: Alloy Phase Diagrams, ASM, Materials Park, Ohio, (1992).

21. Munir, Z. A., Powder Metallurgy World Congress, Vol.9, Metal Powder Industries Federation, American Powder Metallurgy Institute, Princeton, NJ, p.251, (1992).

22. Yi, H. C., A. Petric, and J. J. Moore, Journal of Materials Science, Vol.27, p.6797, (1992).

23. Barin, I., O. Knacke, and O. Kubaschewski, Thermochemical Properties of Inorganic Substances (Supplement), Springer Verlag, Berlin, (1977).

24. Dunand, D. C., Processing and Fabrication of Advanced Materials III, V. A. Ravi, T. S. Srivatsan, and J. J. Moore, eds., TMS, Warrendale, PA, p.771, (1993).

25. Holt, J. B., and Z. A. Munir, Journal of Materials Science, Vol.21, p.251, (1986).

26. Ranganath, S., M. Vijayakumar, and J. Subrahmanyam, Materials Science and Engineering, Vol.A149, p.253, (1992).

27. Subrahmanyam, J., M. Vijaykumar, and S. Ranganath, Metals and Materials Processes, Vol.1, p.105, (1989).

28. Dunand, D. C., J. L. Sommer, and A. Mortensen, Metallurgical Transactions, Vol.24A, p.2161, (1993).

29. Dunand, D. C., J. L. Sommer, and A. Mortensen, Processing and Fabrication

of Advanced Materials for High-Temperature Applications II, V.A. Ravi, and T.S. Srivatsan, eds, TMS, Warrendale, PA, p.635, (1992).

30. Alman, D.E., and N.S. Stoloff, International Journal of Powder Metallurgy, Vol.27, p.29, (1991).
31. Rawers, J. C. and H. E. Maupin, Journal of Materials Science Letters, Vol.12, p.637, (1993).
32. Nishimura, C. and C.T. Liu, Acta Metallurgica et Materialia, Vol.41, p.113, (1993).
33. Nishimura, C. and C. T. Liu, Scripta Metallurgica et Materialia, Vol.26, p.381, (1992).
34. Li, H. P., and J. A. Sekhar, Journal of Materials Research, Vol.8, p.2515, (1993).
35. Lebrat, J. P., A. Varma, and A. E. Miller, Metallurgical Transactions, Vol.23A, p.69, (1992).
36. Lebrat, J. P. and A. Varma, Combustion Science and Technology, Vol.88, p.211, (1993).
37. Jiang, H. G., H. Y. Tong, X. M. Xue, B. Z. Ding, Q. H. Song, Z. Q. Hu, and J. T. Wang, Journal of Materials Science Letters, Vol.12, p.1687, (1993).
38. Ma, E., C. V. Thompson, L. A. Clevenger, and K. N. Tu, Applied Physics Letters, Vol.57, p.1262, (1990).
39. Bose, A., B. Moore, R. M. German, and N. S. Stoloff, Journal of Metals, Vol.40, p.14, (1988).
40. German, R. M. and A. Bose, Materials Science and Engineering, Vol.A107, p.107, (1989).
41. Bose, A., B. H. Rabin, and R. M. German, Powder Metallurgy International, Vol.20, p.25, (1988).
42. Suganuma, K., Materials Letters, Vol.16, p.22, (1993).
43. Song, I. and N.N. Thadhani, Metallurgical Transactions, Vol.23A, p.41, (1992).
44. Horie, Y., R. A. Graham, and I. K. Simonsen, Materials Letters, Vol.3, p.354, (1985).
45. Kesapradist, J., K. Ono, and K. Fukaura, Materials Science and Engineering, Vol.A153, p.641, (1992).
46. Newbery, A. P., B. Cantor, R. M. Jordan, and A. R. E. Singer, Scripta Metallurgica et Materialia, Vol.27, p.915, (1992).
47. Mihelic, B., M. Dakic, R. Djekic, and D. Uskokovic, Materials Letters, Vol.13, p.391, (1992).
48. Mukherjee, S.K., and G.P. Khanra, Journal of Materials Science Letters,

Vol.10, p.1222, (1991).

49. Chen, H., M. Kaya, and R.W. Smith, Materials Letters, Vol.13, p.180, (1992).

50. Mei, B., R. Yuan, and X. Duan, Journal of Materials Research, Vol.8, p.2830, (1993).

51. Dunmead, S. D., Z. A. Munir, J. B. Holt, and D. D. Kingman, Journal of Materials Science, Vol.26, p.2410, (1991).

52. Niedzialek, S. E., G. C. Stangle, and Y. Kaieda, Journal of Materials Research, Vol.8, p.2026, (1993).

53. Henager, C. H., and J. L. Brimhall, Scripta Metallurgica et Materialia, Vol.29, p.1597, (1993).

54. Bowden, D. M., P. J. Meschter, L. H. Yu, M. A. Meyers, and N. N. Thadhani, Journal of Metals, Vol.40, p.18, (1988).

55. Schafrik, R. E., Metallurgical Transactions, Vol.7B, p.713, (1976).

56. Dahms, M., Materials Science and Engineering, Vol.A110, p.L5, (1989).

57. Dahms, M., and S. Schwantes, Materials Science and Engineering, Vol.A151, p.L27, (1992).

58. Wang, G.X., and M. Dahms, Metallurgical Transactions, Vol.24A, p.1517, (1993).

59. Wang, G., and M. Dahms, Journal of Metals, Vol.45, No.5, p.52, (1993).

60. Dogan, B., G.X. Wang, and M. Dahms, Scripta Metallurgica et Materialia, Vol.29, p.943, (1993).

61. Rawers, J. C., W. R. Wrzesinski, E.K. Roub, and R.R. Brown, Materials Science and Technology, Vol.6, p.187, (1990).

62. Rawers, J. C., and W. R. Wrzesinski, Scripta Metallurgica et Materialia, Vol.24, p.1985, (1990).

63. Rawers, J. C., and W. R. Wrzesinski, Journal of Materials Science, Vol.27, p. 2877, (1992).

64. Wrzesinski, W. R., and J. C. Rawers, Journal of Materials Science Letters, Vol.9, p.432, (1990).

65. Misiolek, W., and RM. German, Materials Science and Engineering, Vol.A144, p.1, (1991).

66. Otsuki, M., and N. S. Stoloff, Scripta Metallurgica et Materialia, Vol.26, p.325, (1992).

67. Fukunaga, H., X. Wang, and Y. Aramaki, Journal of Materials Science Letters, Vol.9, p.23, (1990).

68. Ranganath, S., T. L. Prakash, and J. Subrahmanyam, Materials Letters, Vol.10, p.215, (1990).

69. Rabin, B. H., and R. N. Wright,

Metallurgical Transactions, Vol.22A, p.277, (1991).

70. Rabin, B. H., R. N. Wright, J. R. Knibloe, R. V. Raman, and S. V. Rale, Materials Science and Engineering, Vol.A153, p.706, (1992).

71. Wright, J. K., R. N. Wright, and G. A. Moore, Scripta Metallurgica et Materialia, Vol.28, p.501, (1993).

72. Tsunekawa, Y., M. Okumiya, K. Gotoh, T. Nakamura, and I. Niimi, Materials Science and Engineering, Vol.A159, p.253, (1992).

73. Murugesh, L., K. T. V. Rao, and R. O. Ritchie, Scripta Metallurgica et Materialia, Vol.29, p.1107, (1993).

74. Maslov, V. M., I. P. Borovinskaya, and M. K. Ziatdinov, Fizika Goreniya i Vzryva, Vol.15, p.41, (1979).

75. Lu, L., A.B. Gokhale, and R. Abbaschian, Materials Science and Engineering, Vol.A144, p.11, (1991).

76. Murray, J. C., and R. M. German, Metallurgical Transactions, Vol.23A, p.2357, (1992).

77. Bhattacharya, A. K., C. T. Ho, and J. A. Sekhar, Journal of Materials Science Letters, Vol.11, p.475, (1992).

78. Bhattacharya, A. K., Journal of the American Ceramic Society, Vol.75, p.1678, (1992).

9.0 Appendix Headings

Reactants:	initial metallic reactants.
Second phase:	inert or reactive reinforcement added to reactant; *p*: particle, *w*: whisker, and *f*: fiber.
Process:	abbreviations are defined in the text.
Product:	phases after synthesis (minor phases are in parentheses).
Density:	fraction of theoretical density of the equilibrium product.
Mechanical Properties at Room Temp.	TRS: transverse rupture stress YTS: tensile yield stress YCS: compressive yield stress UTS: ultimate tensile stress, UCS: ultimate compressive stress, e: tensile elongation e_c: compressive elongation

Appendix 1. Nickel Aluminides

Reactants	Second Phase	Process	Conditions	Phases	Density	Mechanical Properties	Ref.
Ni+ Al 4.5 at%		RHP	725°C 13 MPa, 1 h	Ni Ni_3Al	< 100%		(31)
Ni+ Al 9.1 at%		RHP	725°C 13 MPa, 1 h	Ni NiAl	< 100%		ibid
3Ni+Al		RS	620°C vacuum	Ni_3Al	96-98%		(32) (33)
3Ni+Al		RHP	620°C 20-150 MPa vacuum	Ni_3Al NiAl Ni	97-99%		ibid
3Ni+Al		SHS	87-417°C air	Al Ni_2Al_3 $NiAl_3$			(34)
Ni 44.5 wt% Fe 35.0 wt% Al 20.5 wt%		SHS	air		57-85%		ibid
3Ni+Al		SHS	vacuum	Ni_3Al NiAl, Ni	75-97%		(35) (36)
3Ni+Al		RA	450°C or 600°C, vacuum	Ni_3Al			(37)
3Ni+Al		RA-SHS	air	Ni_3Al			(38)
Ni+3Al		RA-SHS	air	Al_3Ni Al_3Ni_2, Al			ibid
3Ni+Al		RS	700°C vacuum	Ni_3Al	97%	TRS: 470 MPa UTS: 230 MPa	(39) (40)
3Ni+Al		RHIP	800°C 104 MPa 30 min	Ni_3Al	~100%	UTS: 363 MPa	ibid
3Ni+Al + 0.1 wt% B		RHIP	800°C 104 MPa 30 min	Ni_3Al	~100%	YTS: 265 MPa UTS: 722 MPa e: 10%	ibid

Appendix 1. Nickel Aluminides (continued)

Reactants	Second Phase	Process	Conditions	Phases	Density	Mechanical Properties	Ref.
3Ni+Al + 0.1 wt% B		RHIP	1100°C 172 MPa 1 h		~100%	YTS: 494 MPa UTS: 677 MPa e: 2%	(40)
3Ni+Al		RS	750°C vacuum	Ni_3Al (Ni_5Al_3)	98%		(41)
3Ni+Al		RS	750°C, H_2		97%		ibid
3Ni+Al		RS	750°C, Ar		93%		ibid
3Ni+Al		RS	550-950°C vacuum		90-98%		ibid
3NiAl		RI	Ni: 450-550°C Al: 800°C 50 MPa, air	Ni_3Al	100%	UTS: 400 MPa	(42)
Ni+ Al 44-35 at%		RI	-do-	NiAl Ni_3Al	100%		ibid
3Ni+Al		RSS	> 60 GPa	NiAl Ni_3Al (Ni, Ni_2Al_3)	< 100%		(43)
3Ni+Al		RSS	22 GPa max.	Ni_3Al (NiAl, Ni_2Al_3, $NiAl_3$, Al+Ni)	< 100%		(44)
3Ni+Al+ B 0.26 wt%		RA	1150-1200°C 1-8 h, vacuum	Ni_3Al			(45)
Ni+Al		RSD		Ni_3Al NiAl, Ni_2Al_3 Ni	70-99%		(46)
Ni+ Al 35 at%		RSD		NiAl Ni_3Al	90-99%		ibid
(Ni+NiAl 10%+ Al 49 at%) +		RHIP	1250°C 172 MPa, 4 h	NiAl	100%	YCS: 890 MPa	(30)
Ni+ Al 49 at%		RS	700°C vacuum, 15 min	NiAl	100%	YCS: 544 MPa	ibid
(Ni+Al 49 at%)+ NiAl 15-25%		RS	-do-	NiAl	98%		ibid

Appendix 1. Nickel Aluminides (continued)

Reactants	Second Phase	Process	Conditions	Phases	Density	Mechanical Properties	Ref.
Ni+Al		SHS+ HIP	vacuum 40 MPa	NiAl	< 100%		(47)
Ni+ Al 46-31 at%		RI	Ni: 285-705°C Al: 705-755°C 3.6-6.9 MPa	NiAl Ni_2Al_3 Ni_3Al $NiAl_3$ Ni, Al	< 100%		(28)
3Ni+Al+ B 0.1 wt%	Al_2O_{3f} 3 vol%	RHIP	800°C 104 MPa 30 min	Ni_3Al Al_2O_3	100%	YTS: 474 MPa UTS: 548 MPa e: 1%	(39) (40)
3Ni+Al+ B 0.1 wt%	Y_2O_{3p} 20 vol%	RHIP	800°C 104 MPa 30 min	Ni_3Al Y_2O_3	100%	YTS: 391 MPa UTS: 464 MPa e: 2%	ibid
3Ni+Al+ B 1.5 at%	C_f	RS	620°C nitrogen	Ni_3Al NiAl, C_f			(48)
3Ni+Al% B 0.26 wt%	Al_2O_{3f}	RHP	700°C, 0 MPa, 1 h + 800°C 55 MPa, 1 h vacuum	NiAl Ni_3Al Ni Al_2O_3	< 100%		(45)
3Ni+Al% B 0.26 wt%	Al_2O_{3f}	RHP+ RA	-do-	NiAl Al_2O_3	< 100%		ibid
3Ni+Al	Al_2O_{3f} or TiB_{2p}	RI	Al and Ni: 700-900°C 3.5 MPa vacuum	NiAl Ni_3Al ($NiAl_3$, Al) Al_2O_3 or TiB_2			(49)
3Ni+Al	Al_2O_{3w} 2-10 wt%	SHS		NiAl Ni, Al_2O_3	< 100%		(35)
3Ni+Al (+Cr, Zr, B)	(Ti+C) 35 wt%	SHS		Ni_3Al TiC			(50)
3Ni+Al	(Ti+C) 88-25 wt%	RHP	21 MPa	TiC Ni_3Al	95-98%		(51)

Appendix 1. Nickel Aluminides (continued)

Reactants	Second Phase	Process	Conditions	Phases	Density	Mechanical Properties	Ref.
Ni+Al	-do-	RHP	-do-	TiC, NiAl	94-100%		(51)
5Ni+3Al	(Ti+C) 50 wt%	RHP	-do-	TiC Ni_3Al, NiAl	97%		ibid
2Ni+3Al	-do-	RHP	-do-	TiC, Ni_2Al_3	90%		ibid
Ni+3Al	-do-	RHP	-do-	TiC, Ni_2Al_3 ($NiAl_3$, $TiAl_3$)	93%		ibid
Ni+Al	-do-	RHP	6.9-28 MPa		90-100%		ibid
3Ni+Al	-do-	RHP	-do-		88-100%		ibid
Ni+Al	-do-	RS			55%		ibid
3Ni+Al	-do-	RS			52%		ibid
Ni+Al	(Ti+C) 50 wt%	SHS	vacuum	Ni_xAl_y $Ni_xAl_yTi_z$ NiTi	< 100%		(52)
Ni+Al	(Ti+C+TiC) 50 wt%	SHS	vacuum		< 100%		ibid
3Ni+Al	-do-	SHS	-do-		81-93%		ibid
3Ni+Al	-do-	RHP	350-550°C 11-27 MPa		< 100%		ibid
3Ni+Al	(Ti+C+TiC) 10-90 wt%	RHP	550°C 22 MPa	Ni_3Al TiC (functionally graded)	93%		ibid
(Ni+ Al 49 at%) + NiAl 15%	TiB_2 5 vol%	RS	700°C 15 min vacuum	NiAl TiB_2	94%		(30)
(Ni+ Al 49 at%) + NiAl 15%	TiB_2 10 vol%	RS	-do-	-do-	95%		ibid

Appendix 1. Nickel Aluminides (continued)

Reactants	Second Phase	Process	Conditions	Phases	Density	Mechanical Properties	Ref.
(Ni + Al 49%) + NiAl 15%	TiB_2 15 vol%	RS	700°C 15 min	NiAl TiB_2	86%		(30)
-do-	TiB_2 20 vol%	RS	-do-	-do-	62%		ibid
(Ni + 49 at% Al) + NiAl 10%	TiB_2 15 vol%	RHIP	1250°C 172 MPa, 4 h	NiAl TiB_2	100%	CY: 1060 MPa	ibid
-do-	TiB_2 20 vol%	RHIP	-do-	-do-	100%	CY: 1350 MPa	ibid
-do-	TiB_2 40 vol%	RHIP	-do-	-do-	100%	CY: 1915 MPa	ibid
NiAl	NiO_p 20 mol%	RHP	1300°C 27.5 MPa, 3 h vacuum	NiAl Al_2O_3	100%	TRS: 355 MPa	(53)
NiAl	NiO_p 40 mol%	RHP	-do-	Ni_3Al NiAl, Ni Al_2O_3	95%	TRS: 320 MPa	ibid
Ni+Al	TiAl 70 mol%	RSS			100%		(54)
Ni+ Al 54-43 at%	Al_2O_{3p} 30-34 vol%	RI	Ni: 280-705°C Al: 685-760°C 3.6-6.9 MPa vacuum	NiAl Ni_2Al_3 Ni_3Al $NiAl_3$ Ni, Al	< 100%		(28)

Appendix 2. Titanium Aluminides

Reactants	Second Phase	Process	Conditions	Phases	Density	Mechanical Properties	Ref.
Ti + Al 21 at%		RHP	725°C 13 MPa 1 h	Ti Ti_3Al TiAl	< 100%		(31)
Ti + Al		RS	650°C, 72 h or 993°C, 2 h vacuum	TiAl			(55)
Ti + Al		RS + extrusion	982°C, 8 h 1316-1399°C		91.5-99%		ibid
Ti + Al		RS + extrusion	1000°C, 3.5 h 1427°C	TiAl Ti_3Al (Al_2O_3, TiO)	> 99%	UTS: 214 MPa YCS: 462 MPa e: 0	ibid
Ti + Al		RS + extrusion	640°C, 6.5 h 1316°C		> 99%		ibid
Ti + Al		RA	600°C 23 h, argon	TiAl Ti_3Al	80-95%		(56)
Ti + Al 48 at%		RHIP	1100°C 125 MPa 1 h (uncanned)		~50%		(57)
Ti + Al 48 at%		RHP	540°C 2 MPa, 1 h	Ti Al_3Ti, (Al)	< 100%		ibid
Ti + Al 48 at%		RHP	950°C 2 MPa, 1 h	Ti_3Al TiAl	~100%		ibid
Ti + Al 48 at%		RHIP	1250°C 125 MPa	TiAl Ti_3Al		YTS: 210 MPa YCS: 430-530 MPa	(58)
Ti + Al 48 at%		RA	600°C vacuum, 6 h	TiAl Ti_3Al, $TiAl_2$ $TiAl_3$	68-97%		(59)
Ti + Al 48 at%		RA	1000°C 1350°C	TiAl Ti_3Al	80-97% 84-98%		ibid
Ti + Al 48 at%		RHIP RA+RHIP	1350°C -do-	-do- -do-	93-98% 81-99%		ibid

Appendix 2. Titanium Aluminides (continued)

Reactants	Second Phase	Process	Conditions	Phases	Density	Mechanical Properties	Ref.
Ti+ Al 48 at%		RHIP +RA	1350°C	Ti_3Al	91-95%		(59)
Ti+ Al 48 at%		RHIP	1350°C 110 MPa, 5 h	TiAl		UTS: 375 MPa e: 0%	(60)
Ti+ Al 48 at% + Cr 2%		RHIP	-do-	TiAl(Cr)		UTS: 380 MPa e: 0%	ibid
Ti + Al		SHS		TiAl Ti_3Al $TiAl_3$			(61)
Ti + Al		RHP	1125°C 10 MPa vacuum	TiAl	93%	TRS: 254 MPa	ibid
Ti + Al		RHP	1200°C 1.4-6.5 MPa 15-180 min	TiAl Ti_3Al	91-99%	TRS: 415-1115 MPa	(62) (63)
Ti + Al		RHP	1300°C 6.5-10 MPa 5-15 min	TiAl Ti_3Al	91-98%	TRS: 366-801 MPa	ibid
Ti + Al		RHP	900-1300°C 6.5 MPa 15 min	TiAl Ti_3Al	84-92%	TRS: 149-378 MPa	ibid
Ti + Al 50-60 at%		RHP	1300°C 6.5 MPa 15 min	TiAl Ti_3Al	91-95%	TRS: 320-480 MPa	(63)
Ti + Al		SHS	air vacuum		35%		(64)
Ti + Al		RHIP	1370°C 170 MPa 4 h		100%	UTS: 533 MPa	(65)

Appendix 2. Titanium Aluminides (continued)

Reactants	Second Phase	Process	Conditions	Phases	Density	Mechanical Properties	Ref.
Ti + Al		RS	500-750°C argon	TiAl Ti_3Al ($TiAl_3$)	48-58%		(22)
3Ti + Al		RS	490-660°C argon	Ti_3Al (TiAl+Ti)	65-68%		ibid
Ti + 3Al		RS	540-660°C argon	$TiAl_3$	29-58%		ibid
Ti + Al + TiAl 70 mol%		RSS			100%		(54)
Ti + Al 66 at% + Cr 9 at%		RHIP	1250°C 173 MPa 2 h	$Al_{66}Cr_9Ti_{25}$	100%	CYS: 490 MPa UCS: 1360 MPa e_c: 14%	(66)
Ti + Al 66 at% + Cr 9 at%	Al_2O_{3f} 10 vol%	RHIP	1250°C 173 MPa 2 h	$Al_{66}Cr_9Ti_{25}$ Al_2O_3	100%	CYS: 470 MPa UCS: 1010 MPa e_c: 8%	(66)
Ti + Al 66 at% + Cr 9 at%	Al_2O_{3f} 30 vol%	RHIP	1250°C 173 MPa 2 h	$Al_{66}Cr_9Ti_{25}$ Al_2O_3	100%	CYS: 970 MPa UCS: 1100 MPa e_c: 1.4%	ibid
Ti + Al	B 2-10 mol%	RHP	1300°C 6.5 MPa 15 min	TiAl Ti_3Al TiB_2	> 90%	TRS: 240-410 MPa	(63)
Ti + Al	C 2-10 mol%	RHP	1300°C 6.5 MPa 15 min	TiAl Ti_3Al TiC	> 90%	TRS: 225-450 MPa	ibid
Ti + Al	Si 2-10 mol%	RHP	1300°C 6.5 MPa 15 min	TiAl Ti_3Al Ti_5Si_3	> 90%	TRS: 215-450 MPa	ibid
Ti + Al	Al_2O_3 2-10 mol%	RHP	1300°C 6.5 MPa 15 min	TiAl Ti_3Al Al_2O_3	> 80%	TRS: 161-254 MPa	ibid

Appendix 2. Titanium Aluminides (continued)

Reactants	Second Phase	Process	Conditions	Phases	Density	Mechanical Properties	Ref.
Ti + Al	SiC_p 2-10 mol%	RHP	1300°C 6.5 MPa 15 min	TiAl Ti_3Al Ti_5Si_3 SiC	> 90%	TRS: 157-367 MPa	(63)
Ti + Al	SiC_w 2-10 mol%	RHP	1300°C 6.5 MPa 15 min	TiAl Ti_3Al Ti_5Si_3 SiC	> 90%	TRS: 97-316 MPa	ibid
Ti + Al	B 5 mol%	RHP	1200°C 1.4 MPa	TiAl Ti_3Al TiB	90%		(62)
Ti + Al	C 5 mol%	RHP	1200°C 1.4 MPa	TiAl Ti_3Al TiC	92%		ibid
Ti + Al	Si 5 mol%	RHP	1200°C 1.4 MPa	TiAl Ti_3Al Ti_5Si_3	88%		ibid
Ti + Al	Al_2O_{3p} 2-15 mol%	RHP	900°C 4.1-4.8 MPa vacuum	TiAl (Ti_3Al) Al_2O_3	< 100%	TRS: 31-75 MPa	(64)
Ti + Al	SiC_p 2-15 mol%	RHP	-do-	TiAl (Ti_3Al) Ti_5Si_3	< 100%	TRS: 62-120 MPa	ibid
Ti + Al	SiC 2 mol%	RHP	1200°C 10 MPa vacuum	TiAl Ti_3Al ($Ti_4Al_2C_2$) ($Ti_7Al_5Si_{12}$)	92%	TRS: 372 MPa	(61)
Ti + Al	SiC 5 mol%	RHP	1175°C 10 MPa vacuum	TiAl Ti_3Al Ti_5Si_3 ($Ti_4Al_2C_2$) ($Ti_7Al_5Si_{12}$)	93%	TRS: 607 MPa	ibid

Appendix 2. Titanium Aluminides (continued)

Reactants	Second Phase	Process	Conditions	Phases	Density	Mechanical Properties	Ref.
Ti + Al	SiC 10 mol%	RHP	1220°C 10 MPa vacuum	TiAl Ti_3Al Ti_5Si_3 $(Ti_4Al_2C_2)$ $(Ti_7Al_5Si_{12})$	95%	TRS: 98 MPa	(61)
Ti + Al	SiC 25 mol%	RHP	1190°C 10 MPa vacuum	$Ti_4Al_2C_2$ Ti_5Si_3 (SiC, Al)	96%	TRS: 25 MPa	ibid
Ti + Al	SiC 50 mol%	RHP	1175°C 10 MPa vacuum	$Ti_4Al_2C_2$ SiC Al	94%	TRS: 12 MPa	ibid
Al	TiO_2 16-47 vol%	RI	Al: 800-890°C TiO_2: 340-500°C 50-150 MPa	Al_2O_3 TiAl $TiAl_3$ TiO_2 + Al			(67)

Appendix 3. Iron Aluminides

Reactants	Second Phase	Process	Conditions	Phases	Density	Mechanical Properties	Ref.
3Fe + Al		RS	700°C vacuum	Fe_3Al	54%		(68)
3Fe + Al		RHIP	1000°C 120 MPa 30 min.	Fe_3Al	98%		ibid
Fe + Al 28 at% (+ C)		RS	1000°C vacuum	Fe_3Al (Al_2Fe_6C)	48-75%		(69)
Fe + Al (+C)		RS	-do-	FeAl	54-69%		ibid
Fe + Al 28 at% (+ C)		RHP	1000°C 10-70 MPa argon	Fe_3Al (Al_2Fe_6C)	83-99%	UTS: 840 MPa e: 1.2%	ibid
Fe + Al (+C)		RHP	-do-	FeAl	75-99%		ibid
3Fe + Al (+C)		RHIP	1000-1350°C 138-1242 MPa 1-60 min	Fe_3Al (Al_2Fe_6C)	~100%		(70)
3Fe + Al + Cr 2% (+ C)		RHIP	-do-	Fe_3Al Cr (Al_2Fe_6C)	~100%		ibid
3Fe + Al + Cr 5% (+ C)		RHIP	-do-	Fe_3Al Cr (Al_2Fe_6C)	~100%	YTS: 950 MPa e: 7%	ibid
Fe + Al 28 at%		RHP	1000°C 28 MPa 1 h	Fe_3Al (Al_2Fe_6C)	~100%		(71)
3Fe + Al + Cr 2%		RHP	500°C 20.7 MPa + 1100°C 1 h		~100%		ibid

Appendix 3. Iron Aluminides (continued)

Reactants	Second Phase	Process	Conditions	Phases	Density	Mechanical Properties	Ref.
3Fe + Al B 1 wt% or P 1 wt% or Mg 0.3 wt%		RS	1200°C argon 1 h		< 100%		(71)
Fe + Al		RS	1200°C argon, 1 h		< 100%		ibid
Fe + Al		RHP	1200°C 24.5 MPa 15 min.		< 100%		ibid
Fe + Al + B 1 wt% or P 1 wt% or Mg 0.3 wt%		RS	1200°C argon 1 h		< 100%		ibid
Fe + Al 8.6 at%		RHP	725°C 13 MPa	Fe Fe_3Al Fe_2Al FeAl	< 100%		(31)
3Fe + Al + Cr 0-5% (+ C)	Al_2O_3 10 wt%	RHIP	1000-1100°C 138-207 MPa 1-60 min.	Fe_3Al Cr (Al_2Fe_6C)	100%		(70)
3Fe + Al	N_2	RSD	H_2/N_2 plasma preheated substrate 677°C	Fe_3Al AlN (Fe)	100%		(72)
Fe + Al	N_2	RSD	-do-	FeAl AlN ($FeAl_2$)			ibid
Fe + Al 58-75 at%	N_2	RSD	-do-	Fe_3Al FeAl $FeAl_2$ Fe_2Al_5			ibid

Appendix 4. Niobium and Tantalum Aluminides

Reactants	Second Phase	Process	Conditions	Phases	Density	Mechanical Properties	Ref.
Nb + Al 8 at%		RHP		Nb_3Al Nb		TRS: 460 MPa	(73)
3Nb + Al		RS	750-1000°C inert gas	Nb $NbAl_3$ (Nb_2Al)			(74)
2Nb + Al		RS		$NbAl_3$ Nb_2Al Nb			
Nb + 3 Al		RS		$NbAl_3$			
Nb + 3Al		RHIP	900°C 1 h	$NbAl_3$	100%		(54)
Nb + 3Al		RHP	1350°C 49 MPa 1 h	$NbAl_3$	> 98%		(75)
Nb + 3Al		RS	1200°C 1 h	$NbAl_3$	95%		(65)
		RHIP	1200°C 170 MPa	$NbAl_3$	98%		
Nb + 3Al		RS	800-1400°C 1 h vacuum	$NbAl_3$	48-95%		(76)
Nb + 3Al		RS	1200°C 1 h vacuum	$NbAl_3$	28-82%		
Nb + 3Al		RHIP	1200°C 173 MPa 4 h		> 98%		
Ta + 3 Al		RHIP	1200°C	Al_3Ta (Al_2Ta)	98%	UTS: 531 MPa	(7) (65)

Appendix 4. Niobium and Tantalum Aluminides (continued)

Reactants	Second Phase	Process	Conditions	Phases	Density	Mechanical Properties	Ref.
Ta + 3Al + Fe 8 at%		RHIP	1200°C	Al_3Ta $Ta_xAl_yFe_z$	93%	UTS: 372 MPa	(65)
3Nb + Al	B 3%	SHS	Argon	Nb_2Al (Nb_3Al) (NbB) (Nb)	< 100%		(77) (78)
Nb + Al	TiAl 70 mol%	RSS		TiAl $Ta_xAl_yNb_z$	100%		(54)
Nb + 3Al	Nb 20 vol%	RHP	1350°C 49 MPa 1 h		100%		(75)
Nb + 3Al	Nb 20 vol% (Nb_2O_5)	RHP	1350°C 49 MPa 1 h	Nb $NbAl_3$ (Nb_2Al) (Al_2O_3)	100%		ibid
Nb + 3Al	Al_2O_3 30 vol%	RHIP	1200°C 170 MPa 4 h	$NbAl_3$ Nb_2Al $NbAlO_3$ Al_2O_3	98%		(65) (76)